Measurement of the Strong Coupling α_S from the Four-Jet Rate in e^+e^- annihilation

Jochen Schieck [a]

[a]Max-Planck-Institut für Physik
Föhringer Ring 6, 80805 München, Germany

Data from e^+e^- annihilation into hadrons at centre-of-mass energies between 91 GeV and 209 GeV are used to study the four-jet rate as a function of the Durham algorithm's resolution parameter $y_{\rm cut}$. The four-jet rate is compared to next-to-leading order calculations that include the resummation of large logarithms. The strong coupling measured from the four-jet rate is

$\alpha_s(M_{\rm Z}) = 0.1208 \pm 0.0006(stat.) \pm 0.0021(exp.) \pm 0.0019(had.) \pm 0.0024(scale)$

in agreement with the world average.

1. Introduction

The annihilation of an electron and a positron into hadrons allows a precise test of Quantum Chromodynamics (QCD). Multijet rates are predicted in perturbation theory as functions of the jet-resolution parameter, with one free parameter, the strong coupling $\alpha_{\rm S}$. Calculations beyond leading order are made possible by theoretical developments achieved in the last few years. For multi-jet rates as well as numerous event shape distributions with perturbative expansions starting at $\mathcal{O}(\alpha_{\rm S})$, matched next-to-leading order (NLO) and next-to-leading logarithmic approximations (NLLA) provide very precise description of the data over a wide range of the available kinematic region and centre-of-mass energy [1–4].
In this analysis we use data collected by the OPAL Collaboration at LEP at 13 centre-of-mass energy points covering the full LEP energy range of 91-209 GeV. A more detailed description of the analysis can be found in [5].

2. Observable

Jet algorithms are applied to cluster the large number of particles of an hadronic event into a small number of jets, reflecting the parton structure of the event. For this analysis we use the Durham scheme [2]. The next-to-leading order calculation predicts the four-jet rate R_4, which is the fraction of four-jet events, as a function of $\alpha_{\rm S}$ [6]. The fixed-order perturbative prediction is not reliable for small values of $y_{\rm cut}$. An all-order resummation, given in Ref. [2], is possible for the Durham clustering algorithm. This NLLA calculation is combined with the NLO-prediction using the modified "R matching" scheme described in Ref. [6].

3. Analysis Procedure

The data used in this analysis were collected by OPAL [7] between 1995 and 2000 and correspond to 14.5 $\rm pb^{-1}$ of 91 GeV data, 10.4 $\rm pb^{-1}$ of LEP1.5 data, with centre-of-mass energies $\sqrt{s}$=130 GeV and 136 GeV and 706.4 $\rm pb^{-1}$ of LEP2 data with $\sqrt{s}$=161 to 209 GeV. The highest energy points have a spread of 1-2 GeV and are grouped into the main energy points. The data at 91 GeV were taken during calibration runs at the $\rm Z^0$ peak at the beginning of each year and during data taking in 1996-2000. The breakdown of the data samples, mean $\sqrt{s}$ and collected luminosity are given in Table 1. To study fewer energy points with improved statistical power, we combine the data above 91 GeV into three energy points by taking

luminosity times hadronic cross-section weighted averages of the samples. The LEP1.5 data samples provide an energy point at 133 GeV, while the LEP2 samples give energy points at 178 GeV and 198 GeV corresponding to the energy ranges from 161 to 183 GeV and from 189 to 209 GeV. Samples of Monte Carlo simulated events (JETSET 7.4[8], KK2f[9], PYTHIA 6.125[10], HERWIG 6.2[11], KORALW 1.42[12] and GRC4f[13]) were used to correct the data for experimental resolution, acceptance and backgrounds. The Monte Carlo samples generated at each energy point studied were processed through a full simulation of the OPAL detector [14], and reconstructed in the same way as the data. In addition, for comparisons with the corrected data, and when correcting for the effects of fragmentation, large samples of generator-level Monte-Carlo events were employed, using the parton shower models PYTHIA 6.158, HERWIG 6.2 and ARIADNE 4.11 [15].

3.1. Selection of Events

The selection of events for this analysis consists of three main stages: the identification of hadronic event candidates, the removal of events with a large amount of initial state radiation (ISR), and the removal of four-fermion background events (at energies above the W^+W^- production threshold electroweak four-fermion production becomes a substantial background).
The number of selected candidate events obtained after applying the selection cuts are given in Table 1. After all cuts, the acceptance for non-radiative signal events ranged from 88.5% at 91 GeV to 76.5% at 207 GeV. The residual four-fermion background was negligible below 161 GeV, and increased from 2.1% at 161 GeV to 6.2% at 207 GeV.

3.2. Corrections to the data

The expected number of residual four-fermion background events, was subtracted from the number of data events. The effects of detector resolution, acceptance and of residual ISR were then accounted for by a bin-by-bin correction procedure. The Monte Carlo ratio of the hadron level to the detector level was used as a correction factor for the data.

average energy in GeV	luminosity (pb^{-1})	number of selected events	number of events predicted by Monte Carlo
91.3	14.7	397452	396560.0
130.1	5.31	318	368.4
136.1	5.95	312	329.7
161.3	10.1	281	275.3
172.1	10.4	218	232.2
183.7	57.7	1077	1083.5
188.6	185.2	3086	3130.1
191.6	29.5	514	473.0
195.5	76.7	1137	1161.3
199.5	79.3	1090	1030.8
201.6	38.0	519	526.5
204.9	82.0	1130	1089.6
206.6	137.1	1717	1804.1

Table 1
The average center-of-mass energy and integrated luminosity for each data sample, together with the numbers of selected data and expected Monte Carlo events. The horizontal lines indicate the four energy intervals.

4. Systematic Uncertainties

Several sources of possible systematic uncertainties are studied. We investigate experimental uncertainties, effects due to hadronisation and the theoretical uncertainty, associated with missing higher order terms in the theoretical prediction.

5. Results

5.1. Four-Jet Rate Distributions

The four-jet rates at $\sqrt{s}$=198 GeV after subtraction of background and correction for detector effects is shown in Figure 1. Superimposed we show the predictions by the PYTHIA, HERWIG and ARIADNE Monte Carlo models, which in all cases were tuned to OPAL data at 91 GeV centre-of-mass energy. In order to make a more sensitive

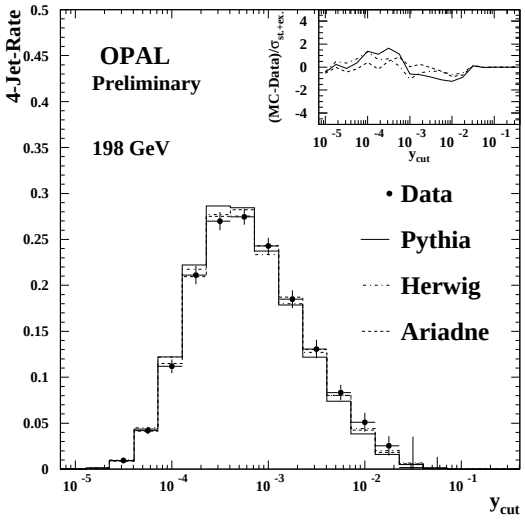

Figure 1. The figures show the four-jet rate distribution at hadron-level as a function of the $y_{\rm cut}$ resolution parameter obtained with the Durham algorithm.

comparison between data and models, the inserts in the upper right corner show the differences between data and each model, divided by the combined statistical and experimental error in that bin. The three models are seen to describe the high energy data at $\sqrt{s}$= 136, 178 and 198 GeV well. However, some minor discrepancies are seen in the data taken at 91 GeV.

5.2. Determination of $\alpha_{\rm S}$

Our measurement of the strong coupling $\alpha_{\rm S}$ is based on the fits of QCD predictions to the corrected four-jet rate distribution. The combined $\mathcal{O}(\alpha_{\rm S}^3)$+NLLA calculation was used. The theoretical predictions of the four-jet rate provide distributions at the parton level. In order to confront the theory with the hadron-level data, it is necessary to correct for hadronization effects. The four-jet rate was calculated at hadron and parton level using PYTHIA and, as a cross-check, with the HERWIG and ARIADNE models. The theoretical prediction is then multiplied by the ratio of the hadron- and parton-level four-jet rates.
A χ^2-value for each energy point is calculated. A single event can contribute to several $y_{\rm cut}$-bins in a four-jet rate distribution and for this reason the bins are correlated and the complete covariance matrix was determined. The χ^2 value is minimized with respect to $\alpha_{\rm S}$ for each energy point separately. The scale parameter is set to unity. The systematic error was determined as described in Section 4. Each distribution was re-fitted and the difference to the default $\alpha_{\rm S}$ value was taken as a symmetric systematic error. The result for

$\sqrt{s}$ GeV	$\alpha_{\rm S}$	stat.	exp.	hadr.	scale
91.3	0.1191	0.0001	0.0010	0.0023	0.0030
134.0	0.1085	0.0038	0.0039	0.0027	0.0035
177.5	0.1094	0.0022	0.0027	0.0013	0.0016
197.2	0.1100	0.0009	0.0025	0.0011	0.0017

Table 2
The mean value of $\alpha_{\rm S}$ for each energy interval, the statistical and experimental errors, and the error due to hadronization and scale uncertainties.

$\alpha_{\rm S}(\sqrt{s})$ and the systematic uncertainties within each energy range are summarized in Table 2. It is also of interest to combine the measurements of $\alpha_{\rm S}$ from the four different centre-of-mass energy points in order to determine a single value. This problem has been subject of extensive study by the LEP QCD working group [16], and we adopt their procedure here.
The set of $\alpha_{\rm S}$ measurements to be combined are first evolved to a common scale, $Q = M_{\rm Z^0}$, assuming the validity of QCD. The measurements are then combined in a weighted mean, to minimize the χ^2 between the combined values and the measurements. The result is $\alpha_s(M_{\rm Z}) = 0.1208 \pm 0.0006(stat.) \pm 0.0021(exp.) \pm 0.0019(had.) \pm 0.0024(scale)$, consistent with the world average value of 0.1172 ± 0.0020 [17]. The average value of $\alpha_{\rm S}$ obtained and the results at each energy point are shown in Figure 2. The hadronization and the scale uncertainty decrease

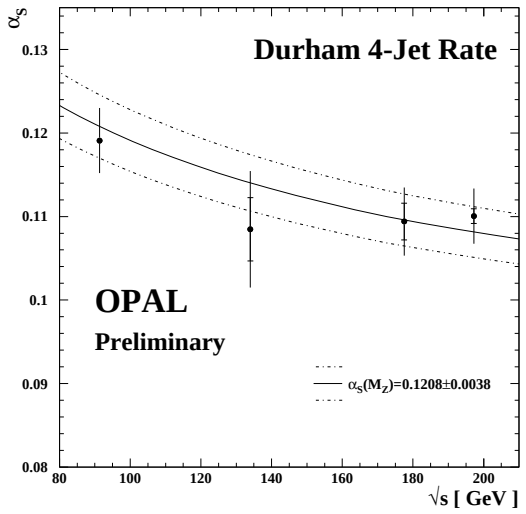

Figure 2. The values for $\alpha_{\rm S}$ in the various energy intervals. The errors show the statistical (inner part) and the total error. The statistical error at 91 GeV is very small and cannot be seen.

with increasing energy. The hadronization scales as an inverse power of $\sqrt{s}$ and the scale uncertainty varies with $\alpha_{\rm S}^3$ so that, for example, a 10% smaller value of α_S at higher energies leads to a 27% smaller scale uncertainty.

6. Summary

In this note we present the preliminary measurements of the OPAL collaboration of the strong coupling from the four-jet rate at centre-of-mass energies between 91 and 209 GeV. The predictions of the PYTHIA, HERWIG and ARIADNE Monte Carlo models are found to be in general agreement with the measured distributions. Some differences are noted in the 91 GeV data where the statistics are largest.
From a fit of $\mathcal{O}(\alpha_{\rm S}^3)$+NLLA predictions to the four-jet rate, we have determined the strong coupling $\alpha_{\rm S}$. The value of $\alpha_s(M_{\rm Z})$ is determined to be $\alpha_s(M_{\rm Z}) = 0.1208 \pm 0.0038$ (total error).

REFERENCES

1. S. Catani *et al.*, *Phys. Lett.* B **263** (1991) 491.
2. S. Catani *et al.*, *Phys. Lett.* B **269** (1991) 432.
3. L. Dixon and A. Signer, *Phys. Rev.* D **56** (1997) 4031.
4. Z. Nagy and Z. Trócsányi, *Nucl. Phys. B (Proc. Suppl.)* **74** (1999) 48.
5. OPAL Collaboration, OPAL Physics Note PN527 (unpublished).
6. Z. Nagy and Z. Trócsányi, *Phys. Rev.* D **59** (1999) 14020.
7. OPAL Collaboration, K. Ahmet *et al.*, *Nucl. Inst. Meth.* **305** (1991) 275.
8. T. Sjöstrand, *Comp. Phys. Comm.* **39** (1986) 347;
   T. Sjöstrand and M. Bengtsson, *Comp. Phys. Comm.* **43** (1987) 367.
9. S. Jadach *et al.*, *Phys. Lett.* B **449** (1999) 97;
   S. Jadach *et al.*, *Comp. Phys. Comm.* **130** (2000) 260.
10. T. Sjöstrand, *Comp. Phys. Comm.* **82** (1994) 74.
11. G. Marchesini *et al.*, *Comp. Phys. Comm.* **67** (1992) 465.
12. S. Jadach *et al.*, *Comp. Phys. Comm.* **119** (1999) 272.
13. J. Fujimoto *et al.*, *Comp. Phys. Comm.* **100** (1997) 128.
14. J. Allison *et al.*, *Nucl. Inst. Meth.* A **317** (1992) 47.
15. L. Lönnblad, *Comp. Phys. Comm.* **71** (1992) 15.
16. R.W.L. Jones *et al.*, paper in preparation.
17. K. Hagiwara *et al.* (particle data group), *Phys. Rev.* D **66** (2002) 010001.